

## 4

## Rotation of the solar interior

JØRGEN CHRISTENSEN-DALSGAARD

*Teoretisk Astrofysik Center, Danmarks Grundforskningsfond, and  
Institut for Fysik og Astronomi, Aarhus Universitet, DK-8000 Aarhus C, Denmark*

MICHAEL J. THOMPSON

*Space & Atmospheric Physics, The Blackett Laboratory, Imperial College,  
London SW7 2BZ, UK*

*Helioseismology has allowed us to infer the rotation in the greater part of the solar interior with high precision and resolution. The results show interesting conflicts with earlier theoretical expectations, indicating that the the Sun is host to complex dynamical phenomena, so far hardly understood. This has important consequences for our ideas about the evolution of stellar rotation, as well as for models for the generation of the solar magnetic field. Here we provide an overview of our current knowledge about solar rotation, much of it obtained from observations from the SOHO spacecraft, and discuss the broader implications.*

**4.1 Introduction**

Solar rotation has been known at least since the early seventeenth century when, with the newly invented telescope, Fabricius, Galileo and Scheiner observed the motion of sunspots across the solar disk (for a brief review, see Charbonneau et al. 1999). The rotation of the Sun and other stars originates from the contracting interstellar gas clouds from which stars are born; these clouds share the rotation of the Galaxy. As the clouds contract, they rotate more rapidly, as a result of the conservation of angular momentum and the reduction in the moment of inertia with contraction (for a discussion of star formation, see Lada & Shu 1990). Although the details of star formation within the contracting clouds are uncertain and involve mass loss and interaction with disks around the star which will transport angular momentum from one part of the cloud to another, it is plausible that newly formed star should be spinning quite rapidly. This is indeed observed: the rotation of the stellar surface causes a broadening of the lines in the star's spectrum,

owing to the Doppler effect, and from measurements of this effect it is inferred that many young stars rotate at near the break-up speed, where the centrifugal force at the equator almost equals gravity.

Stars tend to slow down when they get older. At least for stars of roughly solar type, the observations show that the rotation rate decreases with increasing age (Skumanich 1972). This is thought to take place through angular-momentum loss in a wind, magnetically coupled to the outer parts of the Sun (e.g. Mestel 1968; Mestel & Spruit 1987). The extent to which the slowdown affects the deep interior of the Sun then depends on the efficiency of the coupling between the inner and outer parts. In fact, simple models of the dynamics of the solar interior tend to predict that the core of the Sun is rotating up to fifty times as rapidly as the surface (e.g. Pinsonneault et al. 1989). Such a rapidly rotating solar core could have serious consequences for the tests of Einstein's theory of general relativity based on observations of planetary motion: a rapidly rotating core would flatten the Sun and hence perturb the gravitational field around it. Even a subtle effect of this nature, difficult to see directly on the Sun's turbulent surface, might be significant.

Very detailed observations have been carried out of the solar surface rotation by tracking the motion of surface features such as sunspots and, more recently, by Doppler-velocity measurements. It was firmly established by the nineteenth century, by careful tracking of sunspots at different latitudes on the Sun's surface, that the Sun is not rotating as a solid body: at the equator the rotation period is around 25 days, but it increases gradually towards the poles where the period is estimated to be in excess of 36 days. Figure 4.1 shows the near-surface solar rotation determined from surface Doppler measurements, as well as from tracking magnetic features and large-scale convective flow patterns, as a function of solar latitude. The origin of this *differential rotation* is almost certainly linked to the otherwise dynamic nature of the outer parts of the Sun. In the outer 29 % of the Sun's radius (or 200 Mm), energy is transported by *convection*, in rising elements of warm gas and sinking elements of colder gas: this region is called the *convection zone* (for an overview of solar structure, see Christensen-Dalsgaard et al. 1996). The convection can be seen directly using high-resolution observations of the solar surface, in the *granulation*, with brighter areas of warm gas just arrived at the surface, surrounded by colder lanes of sinking gas. The gas motions also transport angular momentum, and hence provide a link between rotation in different parts of the convection zone. Further-

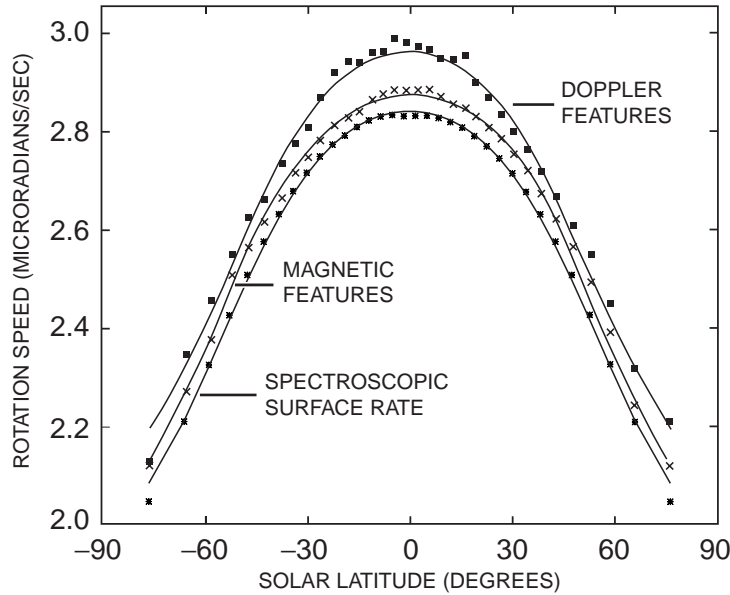


Fig. 4.1. Near-surface solar rotation rates as determined from surface spectroscopic Doppler-velocity measurements, tracking magnetic features, and tracking Doppler features resulting from large-scale convective flow patterns. A rotation period of 36 days corresponds to an angular speed of 2.02 microrad/s, and a period of 25 days corresponds to 2.91 microrad/s. (Adapted from Snodgrass & Ulrich 1990.)

more, convection is affected by rotation, which may introduce anisotropy in the angular momentum transport. Indeed, it is likely that this transport is responsible for the differential rotation, although the details are far from understood.

Similarly complex dynamical interactions are also found in the giant gaseous planets (Jupiter, Saturn, Uranus and Neptune) which, like the Sun, are vigorously convecting as they rotate (see Ingersoll 1990). Here the interaction probably gives rise to the banded structures immediately visible on Jupiter, and more faintly on Saturn. Even closer to home, the Earth's atmosphere and oceans are rotating fluid systems and exhibit, among other things, large-scale circulations and meandering jets such as the jet stream. In all these systems, rotation plays a significant role in the observed dynamical behaviour.

## 4.2 Helioseismic probes of the solar interior

In recent years, the observation that the Sun is oscillating simultaneously in many small-amplitude global resonant modes has provided a new diagnostic of the solar interior. The frequencies of these global modes depend on conditions inside the Sun (Gough & Toomre 1991; see also Chapter 3, by Chitre & Antia), and so by measuring these frequencies we are able to make deductions about the state of the interior. This field is known as *helioseismology*. The observed oscillations are sometimes called five-minute oscillations, because they have periods in the vicinity of five minutes. The modes are distinguished not only by their different frequencies, but also by their different patterns on the surface of the Sun. Specifically, the behaviour of a mode is characterized by a spherical harmonic

$$Y_l^m(\theta, \phi) = c_{lm} P_l^m(\cos \theta) \exp(im\phi) \quad (4.1)$$

as function of co-latitude  $\theta$  and longitude  $\phi$ ; here  $P_l^m$  is a Legendre function, and  $c_{lm}$  is a normalization constant. The spherical harmonics are characterized by two integer numbers, their *degree*  $l$  and their *azimuthal order*  $m$ ; a few examples are illustrated in Fig. 4.2. In addition, a mode is characterized by its radial order  $n$  which, approximately, is given as the number of nodes in the radial direction. The dependence on time  $t$  of the oscillation can be written as  $\exp(-i\omega t)$ , where  $\omega$  is the angular frequency. Different modes are sensitive to different regions of the Sun, depending on their frequency, degree and azimuthal order (see also Chapter 3). In particular, in the radial direction the modes are essentially confined outside an inner *turning point* at the distance  $r = r_t$  from the centre, where  $r_t$  satisfies

$$\frac{c(r_t)}{r_t} = \frac{\omega}{l + 1/2}, \quad (4.2)$$

$c$  being the sound speed; thus low-degree modes extend over much of the Sun while high-degree modes are confined close to the solar surface. By exploiting the different sensitivities of the modes, helioseismology is able to make inferences about localized conditions inside the Sun.

### 4.2.1 Rotational effects on the oscillation frequencies

One of the factors that affect the mode frequencies is the Sun's rotation. The dominant effect of rotation on the oscillation frequencies is quite simple: the oscillation patterns illustrated in Fig. 4.2 actually correspond to waves

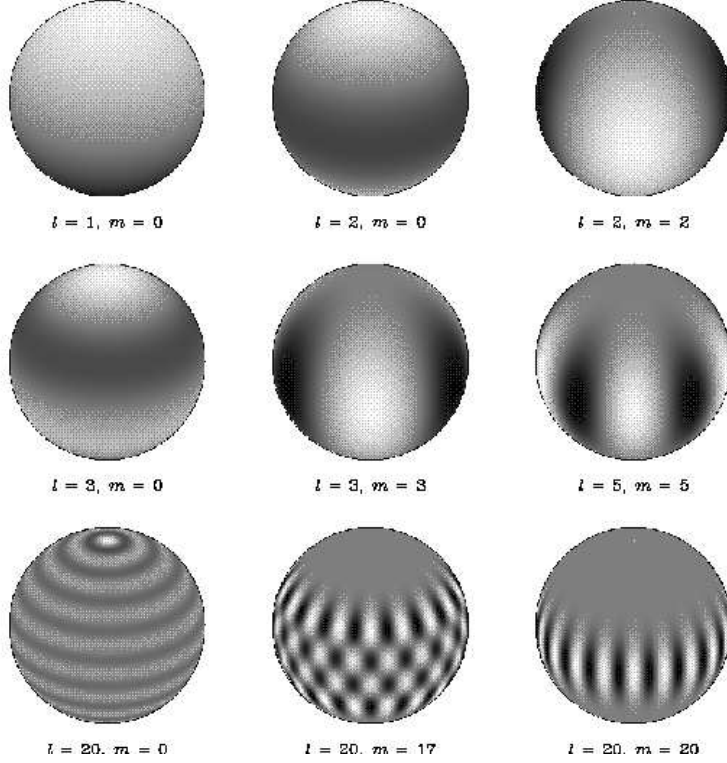


Fig. 4.2. Examples of spherical harmonic patterns, for different values of the degree  $l$  and order  $m$ . For clarity the polar axis has been inclined  $30^\circ$  relative to the page.

running around the equator. Patterns travelling in the same direction as the rotation of the Sun would appear to rotate a little faster, patterns rotating in the opposite direction a little more slowly. When observed at a given position on the Sun the oscillations in the former case would have slightly higher frequency, and in the latter case slightly lower frequency, than if the Sun had not been rotating. The frequency difference between these two cases therefore provides a measure of the rotation rate of the Sun.

This simple description can be made more precise by noting that, as a function of longitude and time  $t$ , the oscillations behave as  $\cos(\omega t - m\phi)$  (apart from an arbitrary phase). We now consider a star that is rotating uniformly, with angular velocity  $\Omega$ , and introduce a coordinate system rotating with the star, with longitude  $\phi'$ ; the longitude  $\phi$  in an inertial frame is related to  $\phi'$  by  $\phi' = \phi - \Omega t$  (cf. Fig. 4.3). We furthermore consider an

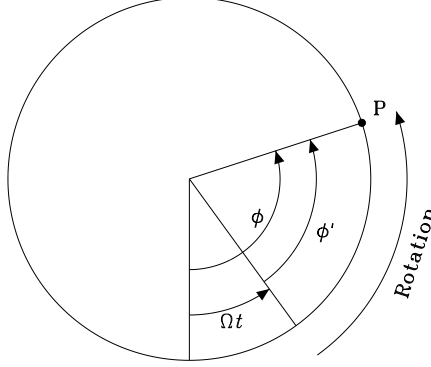


Fig. 4.3. Geometry of rotational splitting, in a star rotating with angular velocity  $\Omega$ . The point  $\mathbf{P}$  has longitude  $\phi'$  in the system rotating with the star and longitude  $\phi = \phi' + \Omega t$  in the inertial system.

oscillation with frequency  $\omega_0$  in the rotating frame, and hence varying as  $\cos(m\phi' - \omega_0 t)$ . Consequently, the oscillation as observed from the inertial frame depends on  $\phi$  and  $t$  as

$$\cos(m\phi - m\Omega t - \omega_0 t) \equiv \cos(m\phi - \omega_m t) ,$$

where

$$\omega_m = \omega_0 + m\Omega . \quad (4.3)$$

Thus the frequencies are split according to  $m$ , the separation between adjacent values of  $m$  being simply the angular velocity; this is obviously just the result of the advection of the wave pattern with rotation.

In reality other effects must be taken into account to describe the frequency shifts caused by rotation, which are often referred to as the *rotational frequency splitting*. The *Coriolis force* affects the dynamics of the oscillations and hence their frequencies, although it turns out that for the modes observed in the five-minute region this effect is modest; owing to the slow rotation of the Sun centrifugal effects are essentially negligible and in any case have a different functional dependence on  $m$  (see Section 5.2.2). However, the variation of angular velocity  $\Omega(r, \theta)$  with position in the Sun must be taken into account<sup>†</sup>. Each mode feels an average angular velocity, where

<sup>†</sup> Specifically,  $\Omega(r, \theta)$  refers to the azimuthal component of the azimuthally averaged flow field within the Sun.

the average is determined by the mode's frequency, degree and azimuthal order (Hansen, Cox & van Horn 1977; Gough 1981). The precise form of this spatial average is described by a weight function, or *kernel*, such that

$$\omega_{nlm} = \omega_{nl0} + m \int_0^R \int_0^\pi K_{nlm}(r, \theta) \Omega(r, \theta) r dr d\theta, \quad (4.4)$$

where  $R$  is the total radius of the Sun; the kernels  $K_{nlm}$  can be calculated from the eigenfunctions for a non-rotating model (Schou, Christensen-Dalsgaard & Thompson 1994). It might be noted that the kernels depend only on  $m^2$ , so that the rotational splitting  $\omega_{nlm} - \omega_{nl0}$  is an odd function of  $m$ . Also, the kernels are symmetrical around the equator; as a result, the rotational splitting is only sensitive to the component of  $\Omega$  which is similarly symmetrical. In the special case where  $\Omega = \Omega(r)$  is independent of  $\theta$ , the integral in Eq. (4.4) is independent of  $m$  and hence the rotational splitting is simply proportional to  $m$ ; note that this is the same linear dependence on  $m$  as for the simple effect of advection (cf. Eq. 4.3).

These weight functions vary from mode to mode. As already indicated in Fig. 4.2, modes with  $m = l$  are concentrated near the equator, increasingly so with increasing  $l$ , whereas modes of lower azimuthal order extend to higher latitudes. Thus modes with  $m = l$  feel an average of the rotation near the equatorial plane, whereas modes of lower azimuthal order sense the average rotation over a wider range of latitudes. In a similar manner, the high-degree five-minute modes (i.e., with large values of  $l$ ) sense only conditions near the surface of the Sun, while modes of low degree feel conditions averaged over much of the solar interior (cf. Eq. 4.2).

These properties can be illustrated by a few examples of weight functions, as shown in Fig. 4.4. The observed modes include some that penetrate essentially to the solar centre, others that are trapped very near the surface, and the whole range of intermediate penetration depths, with a similar variation in latitudinal extent. Thus the observed frequency splittings provide a similarly wide range of averages of the internal rotation.

#### 4.2.2 Data on rotational splitting

The rotational splittings must of course be measured from precise observations of the Sun's global oscillations. Several instruments and observational networks are engaged in this work (see Section 5.3). For practical considerations (including the effects of mode realization arising from the finite lifetime

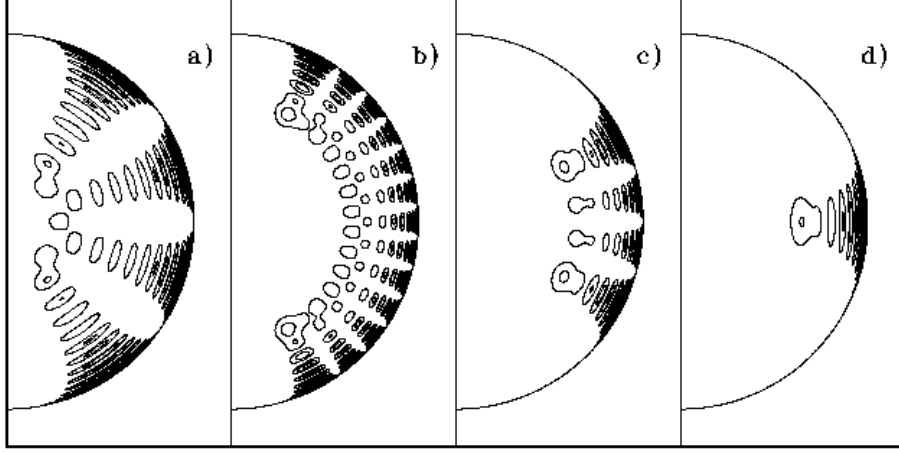


Fig. 4.4. Contour plot of kernel weight functions determining the sensitivity of different modes to the solar internal rotation. All modes have frequencies near 2 mHz; their degree  $l$  and azimuthal order  $m$  are, from left to right:  $(l, m) = (5, 2)$ ,  $(20, 8)$ ,  $(20, 17)$ , and  $(20, 20)$ . Note that the kernels in panels (a) and (b) have roughly the same latitudinal extent, because  $m/(l + 1/2)$  is almost the same for these modes, but the lower- $l$  mode senses the deeper regions of the Sun; also that for fixed  $l$  the modes are more confined to low latitudes as  $m$  increases.

of the modes), the observers commonly do not measure the individual rotational splittings for each  $m$  value but instead fit to the observational data an expression of the form

$$\nu_{nlm} = \nu_{nl0} + \sum_{j=1}^{j_{\max}} a_j(n, l) \mathcal{P}_j^{(l)}(m) . \quad (4.5)$$

Here then the inferred quantities which convey information about the rotation are the so-called  $a$  coefficients  $a_j(n, l)$ , and the  $\mathcal{P}_j^{(l)}$  are polynomials of degree  $j$ , suitably chosen to obtained statistically independent coefficients (cf. Schou et al. 1994). The odd  $a$  coefficients (i.e., odd values of  $j$ ) contain information about the rotation through the advection and Coriolis effects on the modes, and these are used to infer the Sun's internal rotation.

Figure 4.5 shows the first two odd  $a$  coefficients obtained from observations with the SOI-MDI experiment on the SOHO spacecraft. To provide some indication of the variation of rotation with depth, the data are shown against  $\nu/(l + 1/2)$  ( $\nu = \omega/2\pi$  being the cyclic frequency), which according to Eq. (4.2) determines the location of the turning point,  $r = r_t$ , of the mode. The turning-point radius is indicated as the upper abscissas. The increase in  $a_1$

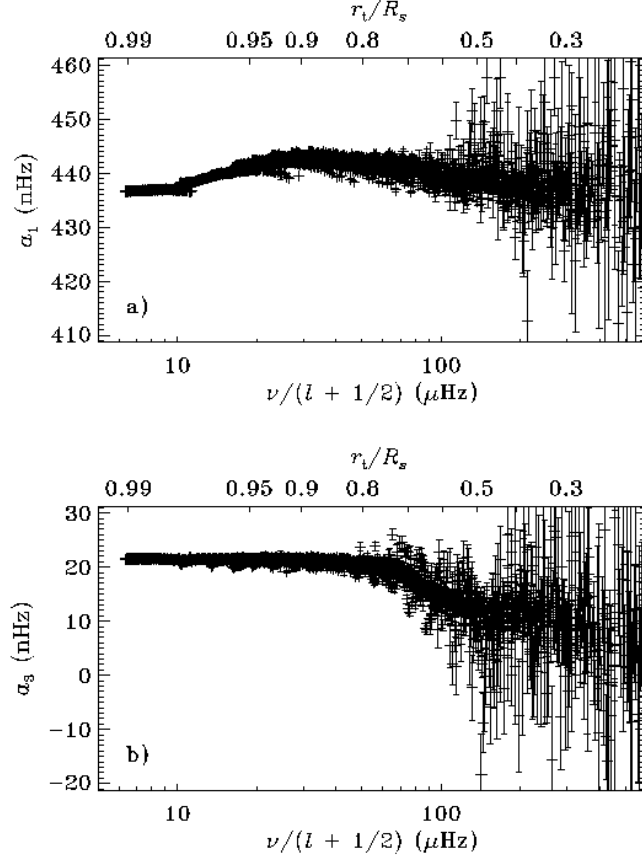


Fig. 4.5. Observed  $a$  coefficients  $a_1$  and  $a_3$  from the expansion given in Eq. (4.5) of frequency splittings from SOI-MDI observations. The error bars correspond to one standard deviation. The upper abscissas indicate the turning-point radius, defined by Eq. (4.2).

with increasing  $\nu/(l + 1/2)$ , i.e., with increasing depth of penetration of the modes, indicates that the rotation rate increases with depth in the outer 5 – 10 % of the solar radius. Also, it should be noticed that  $a_3$  decreases towards zero for those modes that penetrate below  $r = 0.8R$ , as is indeed the case for the higher  $a$  coefficients also; thus the rotational splitting tends to become linear in  $m$ , suggesting that rotation tends towards latitude independence in the inner parts of the Sun (cf. Section 4.2.1). These crude inferences are confirmed by the more detailed analysis presented in Section 4.3.

The even  $a$  coefficients contain information about aspects of the Sun which

affect modes of azimuthal orders  $\pm m$  equally: these include centrifugal distortion and other departures of the Sun from spherical symmetry. The even coefficients are generally small in value and are not used for determining the form of the rotation, though they can be used to make inferences about the Sun's internal asphericity; this is discussed in Chapter 3 of the present volume.

### 4.2.3 *Inversion for solar internal rotation*

The wealth of data on rotational splitting allows the determination of the detailed variation of rotation with position in the solar interior. Modes of high degree, trapped near the surface, provide measures of the rotation of the superficial layers of the Sun. Having determined that, its effect on the somewhat more deeply penetrating modes can be eliminated, leaving just a measure of rotation at slightly greater depths. In this way, information about rotation in the Sun can be ‘peeled’ layer by layer, much as one could an onion, in a way that allows us to obtain a complete image of solar internal rotation.

It is fairly evident that this process gets harder, the deeper one attempts to probe, since fewer and fewer modes penetrate to the required depth; furthermore, the effect of rotation decreases because of the smaller size of the region involved. Thus the rotation of the solar core is difficult to determine. Similarly, all modes are affected by the equatorial rotation while only modes of low  $m$  extend to the vicinity of the poles, and the polar regions have relatively little effect on the oscillations, complicating the determination of the high-latitude rotation. However, as we shall see the quality of current data is such that the angular velocity can be determined quite near the poles, at least in the outer parts of the convection zone.

The analysis of the oscillation data to infer properties of the solar interior is often characterized as *inversion* (Gough & Thompson 1991). To illustrate aspects of these procedures, we write Eq. (4.4) as

$$\Delta_i = \int K_i(\mathbf{x})\Omega(\mathbf{x})d\mathbf{x} , \quad (4.6)$$

where the label  $i$  stands for the modes  $(n, l, m)$  and  $\mathbf{x}$  replaces the coordinates  $(r, \theta)$ ; also,  $\Delta_i = m^{-1}(\omega_{nlm} - \omega_{nl0})$  are the observed data. Likewise, kernels similar to the  $K_i(\mathbf{x})$  can be derived if the data  $\Delta_i$  are in the form of  $a$  coefficients, as in Eq. (4.5). The goal of the analysis is obviously to infer the

properties of  $\Omega(\mathbf{x})$  from the data, taking into account also the observational errors. In most cases considered so far, the analysis corresponds either implicitly or explicitly to making linear combinations of the data; thus to infer  $\Omega$  at a point  $\mathbf{x}_0 = (r_0, \theta_0)$ , say, coefficients  $c_i(\mathbf{x}_0)$  are determined such that, as far as possible,

$$\Omega(\mathbf{x}_0) \simeq \bar{\Omega}(\mathbf{x}_0) = \sum_i c_i(\mathbf{x}_0) \Delta_i , \quad (4.7)$$

where  $\bar{\Omega}$  is the inferred approximation to the true angular velocity. From Eq. (4.6) it then follows that

$$\bar{\Omega}(\mathbf{x}_0) = \int \mathcal{K}(\mathbf{x}_0, \mathbf{x}) \Omega(\mathbf{x}) d\mathbf{x} , \quad (4.8)$$

where the *averaging kernels*  $\mathcal{K}$  are given by

$$\mathcal{K}(\mathbf{x}_0, \mathbf{x}) = \sum_i c_i(\mathbf{x}_0) K_i(\mathbf{x}) . \quad (4.9)$$

Also, if the standard errors  $\sigma(\Delta_i)$  of the observations are known, the error in the inferred angular velocity  $\bar{\Omega}(\mathbf{x}_0)$  can be found from Eq. (4.7).

It is evident from Eq. (4.8) that the coefficients  $c_i(\mathbf{x}_0)$  should be determined such that  $\mathcal{K}(\mathbf{x}_0, \mathbf{x})$  is as far as possible localized near  $\mathbf{x} = \mathbf{x}_0$ . The extent of  $\mathcal{K}$  provides a measure of the resolution of the inversion. At the same time, it must be ensured that the error on  $\bar{\Omega}(\mathbf{x}_0)$  is reasonable. In general, there is a trade-off between error and resolution, determined by one or more parameters of the procedure.

In one commonly used inversion procedure, the so-called regularized least-squares (or RLS) procedure, the solution is parametrized and the parameters are determined through a least-squares fit of the data to the right-hand side of Eq. (4.6). To ensure that the solution is well-behaved and the errors are of reasonable magnitude, the fit is regularized by limiting also, for example, a measure of the square of the second derivative of the solution, thus penalizing rapid variations. From the results of the fit the coefficients  $c_i(\mathbf{x}_0)$ , and hence the averaging kernels, can be determined. In a second class of procedures, the optimally-localized averages (or OLA) procedures, the  $c_i(\mathbf{x}_0)$  are determined such as to obtain a localized averaging kernel  $\mathcal{K}(\mathbf{x}_0, \mathbf{x})$ , while at the same time limiting the errors. Details of these procedures and their results were given by Schou et al. (1998).

As already remarked, the weight functions (Fig. 4.4) are symmetrical around the solar equator, and so we can infer only the similarly symmetric

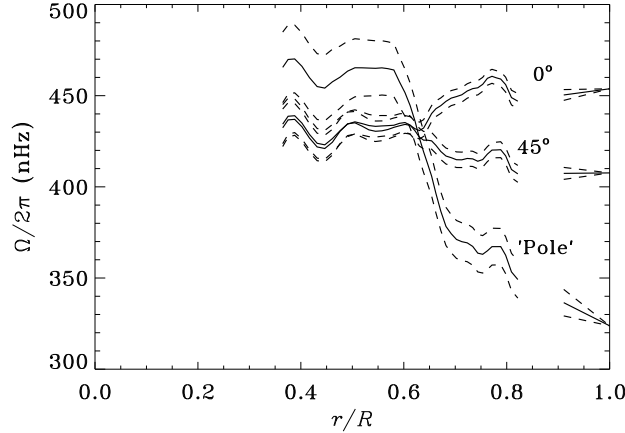


Fig. 4.6. Rotation rate  $\Omega/2\pi$  inferred from inversion of  $a$  coefficients from BBSO (Libbrecht 1989), targeted at the equator, latitude  $45^\circ$  and the pole. The dashed lines indicate the  $1 - \sigma$  error limits. The inversion was only possible between  $0.4R$  and  $0.8R$ ; for clarity, the results have been connected with the directly observed surface rates. (Adapted from Christensen-Dalsgaard & Schou 1988.)

component of rotation. This must be kept in mind in the following, when interpreting the results. We note that this restriction can be avoided by applying *local helioseismology* techniques to the data: such techniques are described elsewhere in this volume by Kosovichev.

### 4.3 The solar internal rotation

Early helioseismic data on rotational splittings provided information only about the modes with  $m \simeq \pm l$ ; as a result, they were sensitive mainly to rotation near the equator. Duvall et al. (1984) showed that there was relatively little variation of rotation with depth; in particular, there were no significant indications of a rapidly rotating core. A few years later initial data on the dependence of the splitting on  $m$  were obtained (Brown 1985; Libbrecht 1988, 1989). Strikingly, they indicated that the surface latitudinal differential rotation persisted through the convection zone, whereas there was little indication of variation with latitude in the rotation beneath the convection zone (e.g. Brown & Morrow 1987; Brown et al. 1989; Christensen-Dalsgaard & Schou 1988; see also Fig. 4.6).

In the last few years the amount and quality of helioseismic data on solar

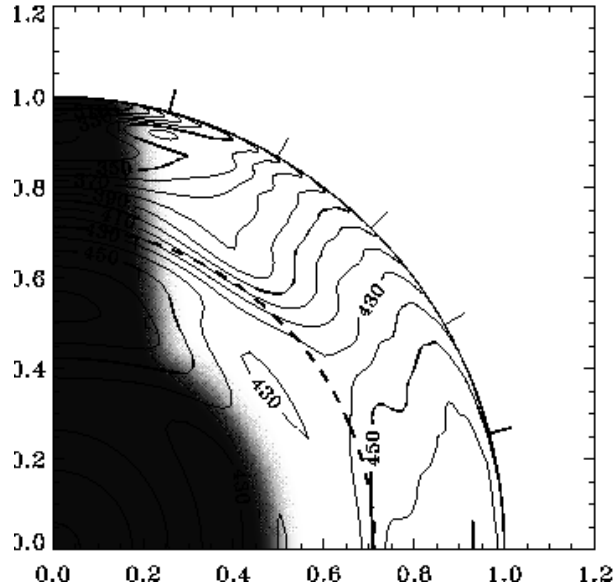


Fig. 4.7. Rotation of the solar envelope inferred from observations by SOI-MDI (Schou et al. 1998). The equator is at the horizontal axis and the pole is at the vertical axis, both axes being labelled by fractional radius. Some contours are labelled in nHz, and, for clarity, selected contours are shown by bolder curves. The dashed circle indicates the base of the convection zone and the tick marks at the edge of the outer circle are at latitudes  $15^\circ$ ,  $30^\circ$ ,  $45^\circ$ ,  $60^\circ$ , and  $75^\circ$ . The shaded area indicates the region in the Sun where no reliable inference can be made with the current data.

rotation have increased dramatically, as a result of several ground-based and space-based experiments (Duvall 1995). The LOWL instrument of the High Altitude Observatory has provided high-quality data on modes of low and intermediate degree over the past more than five years. The BiSON and IRIS networks, observing low-degree modes in Doppler velocity integrated over the solar disk, have yielded increasingly tight constraints on the rotation of the solar core, while the GONG six-station network is setting a new standard for ground-based helioseismology (Harvey et al. 1996). Further, the SOI-MDI experiment on SOHO (Scherrer et al. 1995) has yielded a wealth of data on modes of degree up to 300, allowing a detailed analysis of the properties of rotation in the convection zone. The results we present below are the combined knowledge that has emerged from these observational efforts (e.g. Tomczyk, Schou & Thompson 1995; Thompson et al. 1996; Corbard et al.

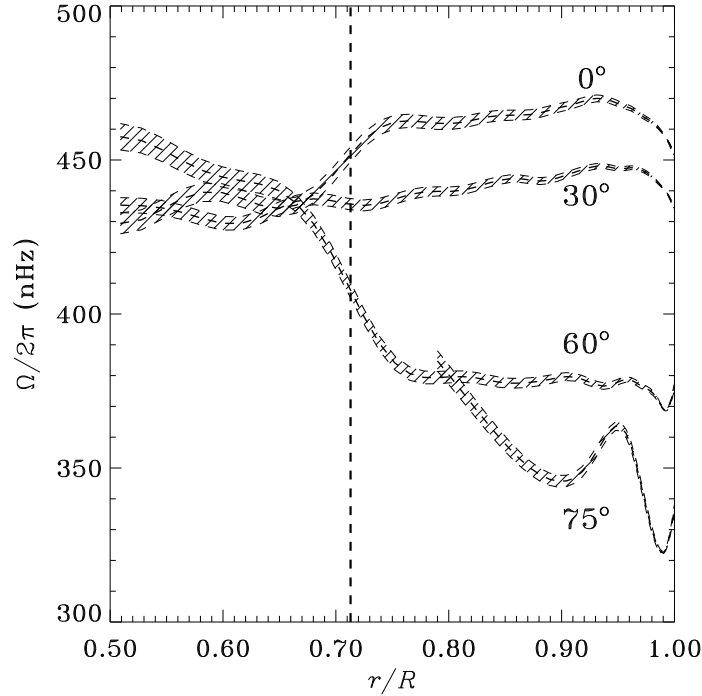


Fig. 4.8. Rotation of the solar envelope as a function of radius, at the latitudes indicated, inferred from observations by SOI-MDI (Schou et al. 1998). The heavy dashed line marks the base of the convection zone.

1997, 1999; Di Mauro & Dziembowski 1998; Schou et al. 1998). Some of these results are illustrated in Figs 4.7 and 4.8. These are the result of a so-called regularized least squares inversion applied to SOI-MDI data (Schou et al. 1998). Figure 4.7 shows the inferred rotation as a contour plot, in the region where the results are judged to be reliable; Fig. 4.8 shows the radial cuts through the same solution, at a few selected latitudes.

#### 4.3.1 Rotation of the solar convection zone

In discussing what we now know about the rotation inside the Sun, we shall start from the near-surface layers and work towards the centre. As we have already discussed, the outer 29 per cent of the Sun is convectively unstable. Before helioseismology, models predicted that the rotation inside the convection zone would organize itself on cylinders aligned with the rotation

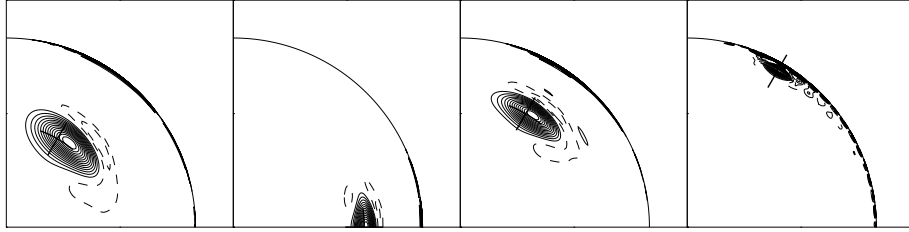


Fig. 4.9. Averaging kernels for the inversion solution shown in Fig. 4.7, at selected radii and latitudes in the Sun, which are (from left to right) as follows:  $0.540R$ ,  $60^\circ$ ;  $0.692R$ ,  $0^\circ$ ;  $0.692R$ ,  $60^\circ$ ;  $0.952R$ ,  $60^\circ$ . The corresponding locations are indicated with crosses. Positive contours are shown as solid lines, negative contours as dashed lines. (Adapted from Schou et al. 1998.)

axis (Glatzmaier 1985; Gilman & Miller 1986; see also Section 4.4). Thus the rotation at depth at, say, equatorial latitudes would match the surface rotation at high latitudes, rather than the faster equatorial rotation at the surface, and so at given latitude the rotation in the convection zone would decrease with depth. Helioseismology has shown that this is not so: to a first approximation it is more accurate to say that the rotation at a given latitude is nearly constant with depth, or to put it another way the differential rotation seen at the surface imprints itself through the convection zone. This finding is clearly visible in Figs 4.7 and 4.8. In detail, the situation is more complicated. At low latitudes, immediately beneath the solar surface the rotation rate actually initially *increases* with depth. The equatorial rotation reaches a maximum at a depth of about 50 Mm (i.e., about 7 per cent of the way in from the surface to the centre of the Sun): at this point, the rotation rate is about 5 per cent higher than it is at the surface. This is consistent with a variety of surface measurements of rotation. Tracking sunspots tends to give a slightly higher rotation rate than that obtained by making direct spectroscopic measurements of the velocity of the surface (Korzennik et al. 1990; see also Fig. 4.1). Probably the reason is that the sunspots extend to some depth below the surface, and so are dragged along at a rate that is more similar to the subsurface rotation a few per cent beneath the surface which helioseismology has revealed.

Figure 4.9 shows averaging kernels (cf. Eq. 4.9) corresponding to the solution in Fig. 4.7, at a few locations inside the Sun. These give an indication of the resolution attained by the inversion. Note that the radial resolution is finer for points high in the convection zone and poorer in the radiative

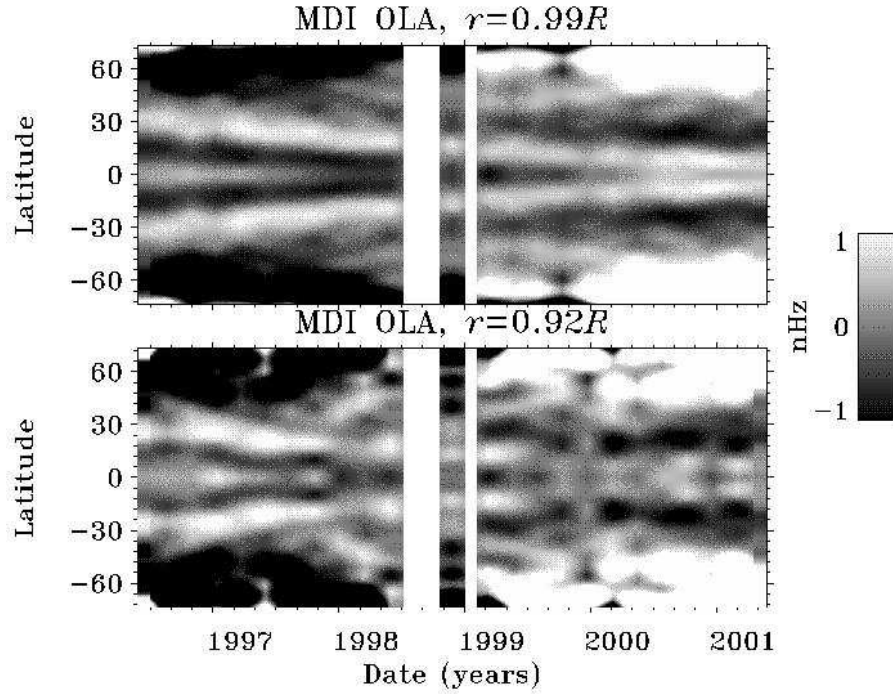


Fig. 4.10. The evolution with time of the fine structure in the near-surface solar rotation, based on observations from the SOI-MDI instrument on the SOHO spacecraft, after subtraction of the time-averaged rotation rate. The result is represented as a function of time (horizontal axis) and latitude (vertical axis), the grey scale at the right giving the scale in nHz; 1 nHz corresponds to a speed of around 4 m/s at the equator. The banded structure, apparently converging towards the equator as time goes by, should be noted. The vertical white bands correspond to time intervals when the spacecraft was temporarily inactive. (Adapted from Howe et al. 2001.)

interior. This is largely a reflection of the local vertical wavenumber of the waves at the various depths.

The rotational velocity at the surface of the Sun is about 2 km per second, dropping off rather smoothly towards higher latitudes. However, it has now been found that superimposed on this are bands of faster and slower rotation, a few metres per second higher or lower than the mean flow (Kosovichev & Schou 1997; Schou 1999). The origin of this behaviour, illustrated in Fig. 4.10, is not understood, but it is reminiscent of the more pronounced banded flow patterns seen on Jupiter and Saturn. Evidence for such bands

had been obtained previously from direct Doppler measurements on the solar surface (Howard & LaBonte 1980). However, the seismic inferences have shown that they extend to a depth probably exceeding 40 Mm beneath the surface (Howe et al. 2000a). Moreover, these bands migrate from high latitudes towards the equator over the solar cycle.

It has been customary to represent the directly measured surface rotation rate in terms of a simple low-order expansion in  $\sin \psi$ , where  $\psi$  is latitude on the Sun. This in fact quite successfully captured the observed behaviour; however, since the solar rotation axis is close to the plane of the sky, direct measurements of rotation near the poles are difficult and uncertain. Strikingly, the helioseismic results have shown a marked departure from this behaviour, at latitudes above about  $60^\circ$ : Relative to the simple fit, the actual rotation rate decreases quite markedly there. The origin or significance of this behaviour is not yet understood. There is also evidence, hinted at in Fig. 4.7, of a more complex behaviour of rotation at high latitudes. Some analyses have shown a ‘jet’, i.e., a localized region of more rapid rotation, at a latitude around  $75^\circ$  and a depth of about 35 Mm beneath the solar surface (Schou et al. 1998). Also, evidence has been found that the rotation rate shows substantial variations in time at high latitudes, over time scales of order months. It is probably fair to say that the significance of these results is still somewhat uncertain, however. Also, it should be kept in mind, as mentioned above, that the results provide an average of rotation in the Northern and Southern hemispheres and, evidently, an average over the observing period of at least 2 – 3 months. Thus the interpretation of the inferred rotation rates in terms of the actual dynamics of the solar convection zone is not straightforward.

#### 4.3.2 The tachocline

At the base of the convection zone, a remarkable transition occurs: the variation of rotation rate with latitude disappears, so that the region beneath the convection zone rotates essentially rigidly, at a rate corresponding to the surface rate at mid-latitudes (see Fig. 4.12). The region over which the transition occurs is very narrow, no more than a few per cent of the total radius of the Sun (e.g. Kosovichev 1996, Charbonneau et al. 1999). This layer has been called the *tachocline* (Spiegel & Zahn 1992). Why the differential rotation does not persist beneath the convection zone is not yet

known, but it is possible that a large-scale weak magnetic field permeates the inner region and enforces nearly rigid rotation by dragging the gas along at a common rate (Gough & McIntyre 1998). Such a field is quite possible as a relic from the original collapsing gas cloud from which the Sun condensed.

The discovery of the tachocline, and of the form of the rotation in the convection zone, has led to an adjustment of our theories of the *solar dynamo* (see the chapter by Choudhuri in this volume). One idea is that the dynamo action consists of two components: a twisting of the magnetic field by the motion of convective elements, and a shearing out of the field by differential rotation. Prior to the helioseismic findings, the simulations of rotation implied that the radial gradient of differential rotation in the convection zone could provide the second ingredient, so it was thought that the dynamo action occurred in that region. Now, however, the tachocline with its very substantial radial gradient seems a more likely location for the dynamo action producing the large-scale magnetic field (Gilman, Morrow & DeLuca 1989).

If the magnetic field is built up in the tachocline over the course of the solar cycle, one might expect to see variations over time in the tachocline properties, including perhaps the rotation rate there. Variations in the rotation rate have in fact been found in the vicinity of the tachocline, but the timescale was unexpected. Rather than the 11-year timescale of the solar cycle, Howe et al. (2000b) have reported quasi-periodic variations in the equatorial region just above and below the tachocline with a period of 1.3 years (Fig. 4.11). The oscillations are revealed by subtracting out the temporal mean rotation rate at each location and looking at the residuals as a function of time. The equatorial variations at radius  $0.72R$  show the 1.3-year oscillation most strongly, and the variations at radius  $0.63R$  exhibit the same period but are in antiphase. This implies that the radiative interior also partakes in the temporal variation, and suggests perhaps a back-and-forth exchange of angular momentum between the two locations. The signal is much weaker at  $30^\circ$  latitude, and the variations at higher latitudes are possibly not significant. These findings are exciting because they may represent the first direct observation of variability at the seat of the solar dynamo.

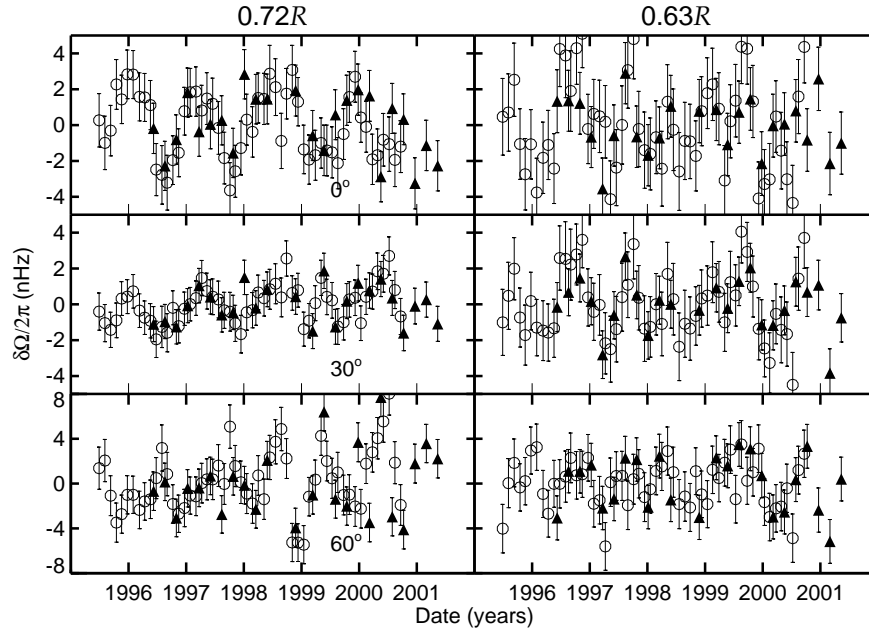


Fig. 4.11. Deviation from the mean rotation rate inferred from inversions at various locations near the base of the convection zone, as a function of time. Open circles represent results from the GONG network, and filled triangles are from the SOI-MDI experiment. (From Howe et al. 2001.)

#### 4.3.3 The radiative interior

Even deeper in the Sun, in the radiative interior, the helioseismic results on the rotation are more uncertain due to the fact that so few of the observed five-minute modes (only the low-degree modes) have any sensitivity to this region. Indeed, the results have been somewhat contradictory (for a review, see Eff-Darwich & Korzennik 1998), some indicating rotation faster than the surface rate and others indicating rotation slower than or comparable to the rotation rate at the base of the convection zone; an example is illustrated in Fig. 4.12. However, down to within 15 per cent of the solar radius from the centre, which is the deepest point at which present observations permit localized inferences to be made, all the modern results agree that the rotation rate is not more than a factor two different from the surface rate: thus early models which predicted that the whole of the nuclear-burning core was rotating much faster are firmly ruled out. Again, this finding would be

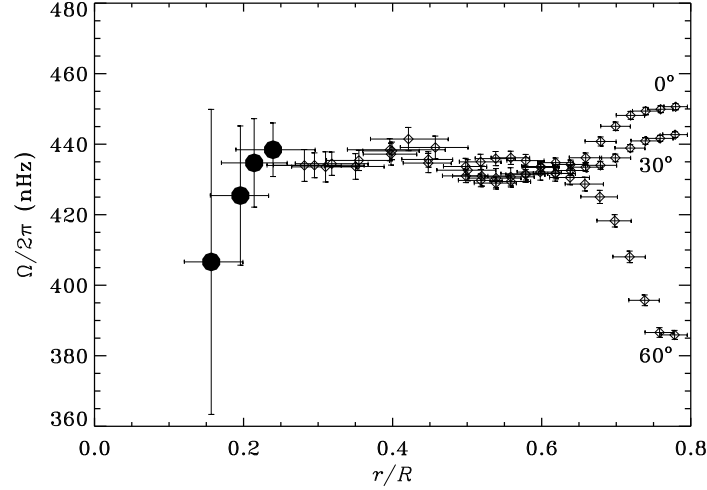


Fig. 4.12. The inferred rotation as a function of fractional radius inside the Sun at three solar latitudes: the equator,  $30^\circ$  and  $60^\circ$ ; the vertical axis shows the rotation frequency in nHz. The vertical error bars indicate the statistical uncertainty on the rotation rate ( $\pm 1$  standard deviation), whereas the horizontal bars provide a measure of the radial resolution of the inversion. Note that the result becomes much more uncertain in the deep interior, where furthermore the different latitudes cannot be separated. The observations used to infer the rotation were from the LOWL instrument and the BiSON network (Chaplin et al. 1999).

consistent with a magnetic field linking the core to the bulk of the radiative interior.

#### 4.4 Modelling solar rotation

Although helioseismology has provided us with a remarkably detailed view of solar internal rotation, the theoretical understanding of the inferred behaviour is still incomplete. In the convection zone, the problem is to model the complex combined dynamics of rotation and convection, the latter occurring on scales from probably less than a few hundred kilometres to the scale of the entire convection zone and time scales from minutes to years. Viscous dissipation is estimated to occur on even smaller spatial scales, of order 0.1 km or less. Capturing this range of scales is entirely outside the possibility of current numerical simulations; thus simplifications are required. Detailed simulations of near-surface convection, on a scale of a few

Mm, have been remarkably successful in reproducing the observed properties of the granulation (Stein & Nordlund 1989, 1998) but are evidently not directly relevant to the question of rotation. Simulations of the entire convection zone are necessarily restricted to rather large scales and hence cannot capture the near-surface details. Such simulations, therefore, typically exclude the outer 30 Mm of the convection zone. Early examples of such simulations by Gilman and Glatzmaier, of fairly limited resolution, showed a tendency for rotation to organize itself on cylinders (Glatzmaier 1985; Gilman & Miller 1986): the rotation rate depended primarily on the distance to the rotation axis. The convection itself in these simulations was dominated by so-called *banana cells* – long, thin, large-scale convection cells oriented in the north-south direction – as seen also, for example, in laboratory convection as observed in the GFFC Spacelab experiment (Hart et al. 1985).

Rotation on cylinders is predicted for simple systems by the *Taylor-Proudman theorem*, which may be derived as follows. The velocity  $\mathbf{u}$  in an inviscid fluid in a gravitational potential  $\Phi$  satisfies an equation of motion

$$\frac{\partial \mathbf{u}}{\partial t} + \mathbf{u} \cdot \nabla \mathbf{u} = -\frac{1}{\rho} \nabla p - \nabla \Phi, \quad (4.10)$$

where  $p$  and  $\rho$  are pressure and density respectively, and  $t$  is time. Suppose that the velocity is purely rotational and independent of time, so in cylindrical coordinates  $(s, \phi, z)$  we write  $\mathbf{u} = s\Omega(s, z)\mathbf{e}_\phi$ , where  $s$  is the distance from the rotation axis,  $z$  distance along the axis, and  $\mathbf{e}_\phi$  is a unit vector in the azimuthal direction. Taking the curl of Eq. (4.10) gives

$$-s \frac{\partial \Omega^2}{\partial z} \mathbf{e}_\phi = \frac{1}{\rho^2} \nabla \rho \times \nabla p. \quad (4.11)$$

In the solar convection zone the fluid is essentially isentropic (uniform specific entropy) and so the pressure can be regarded as a function of the density alone: hence the right-hand side of Eq. (4.11) is zero, and thus  $\Omega$  depends only on  $s$ , not on  $z$ , i.e., the rotation rate is uniform on cylindrical surfaces.

If the Taylor-Proudman theorem applied in the Sun, the rotation rate on a given cylinder would obviously be observable where the cylinder intersected the surface; thus the observed decrease of rotation rate with increasing latitude would correspond to a similar decrease of rotation rate with depth at, say, the equator. The actual solar rotation, shown in Fig. 4.7, is obviously very different from this behaviour and from the simulation results men-

tioned above. The overall variation of rotation within the convection zone is evidently predominantly with latitude, with little variation in the radial direction except in the tachocline. Given the necessary simplifications of the calculations, their failure to model solar rotation is perhaps not surprising. In particular, the effects of smaller-scale turbulence (beneath the smallest scale resolved in the simulation) is typically represented as some form of viscosity; it was suggested by Gough (1976), and later by others, that the effect of rotation on the small-scale motion might render this turbulent viscosity non-isotropic, with important effects on the transport of angular momentum within the convection zone. Of course, such effects were not included in our derivation of the Taylor-Proudman theorem, where the inviscid fluid equations were used and the flow was assumed to be described just by the (large-scale) rotation. In contrast, simple models of convection-zone dynamics, with parametrized anisotropic viscosity, have in fact had some success in reproducing the helioseismically inferred rotation rate (Pidatella et al. 1986).

Recent advances in computing power have led to improved numerical simulations (Miesch et al. 2000; Brun & Toomre 2001), which come closer to representing turbulent convective flow regimes such as exist in the Sun's convection zone. Figure 6 shows results from two such simulations by Miesch, Elliott and Toomre. The simulations can yield a range of differential rotation profiles, depending on the conditions imposed at the top and bottom boundaries of the simulation region, and on the parameter values adopted for the problem. Since it is not obvious what are the most appropriate boundary conditions and parameter values to choose, it is necessary to explore various possibilities and study the different responses. Simulation B has rotation contours at mid-latitudes which are nearly radial, as in the Sun (compare Fig. 4.7), but the contrast in rotation rate between low and high latitudes is not as great as is observed in the Sun (about 70 nHz, rather than 130 nHz). In case A, the latitudinal variation of the Sun's rotation is better reproduced, but the mid-latitude contours do not look quite as similar to those in Fig. 4.7. Nonetheless these results are encouraging indications that we may be close to reproducing theoretically the gross features of the solar rotation inferred by helioseismology. There is still though much work ahead, both observational and theoretical, in getting a detailed understanding of the Sun's rotation and with that, we hope, a better understanding of the

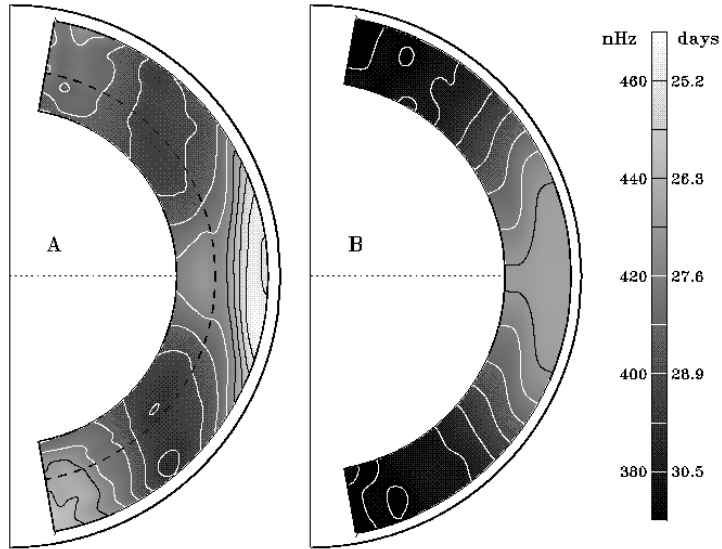


Fig. 4.13. The results of two simulations of convection-zone rotation by Miesch, Elliott and Toomre (Miesch 2000). The two simulations use different boundary conditions and parameter values, and illustrate some of the range of possible responses of the differential rotation to the form of the convection. Also note that Simulation A has a higher resolution and includes penetration into a stable region beneath the convection zone, whereas the convective motions in Simulation B are more laminar and there is no penetration beneath the convection zone.

solar activity cycle and of large-scale rotating fluid systems on planets and stars.

#### 4.5 Final remarks

The advent of helioseismology has revolutionized our knowledge of the Sun's internal rotation, showing that the dynamics of the solar interior are quite different from the pre-helioseismic model simulations. The rotation within the convection zone is now well established except perhaps at high latitudes, and the more turbulent simulations appear to be getting close to matching observation. The existence of the tachocline and the near-uniform rotation in much of the deeper interior are also well established, and suggest that a magnetic field enforces essentially rigid rotation in at least the outer part of the Sun's radiative interior. The rotation of the very deepest part of the Sun is still somewhat uncertain but a very fast-spinning core is ruled out unless

it is very small. The temporal variations of the near-surface banded flows are firmly established but their origin is still incompletely understood. The less certain aspects of the helioseismic inferences are the temporal variations around the tachocline region and the high-latitude jet: we must wait to see whether these are confirmed by future observations.

In addition to the global helioseismic investigations, the newer field of local helioseismology (described more fully in the chapter by Kosovichev) is providing knowledge of the dynamics of the near-surface layers of the Sun. These techniques, which by virtue of their local character can also provide information about how flows and structure vary with longitude and in the northern and southern hemispheres, reveal not only the rotational flow field, but also meridional (i.e., North-South) flows. Meridional flows are likely to play a significant role in understanding the angular-momentum budget in the convective envelope. Recent findings with one such local helioseismic technique (Haber et al. 2001) indicate fascinating changes in the structure of the meridional circulation patterns in one hemisphere of the Sun from year to year; also, they confirm the migrating banded flows in the near-surface rotation but indicate that they can be markedly asymmetric about the equator. These near-surface findings, combined with the deeper inferences of the global methods, continue to provide an intriguing insight into the dynamics of the solar interior.

*Acknowledgements* We are grateful to Prof. R. K. Ulrich for providing Fig. 4.1, to Dr. R. Howe providing Figs 4.10 and 4.11, and to Dr. M. Miesch for providing Fig. 4.13. We are happy to acknowledge the financial support of the UK Particle Physics and Astronomy Research Council, and the Danish National Research Foundation through its establishment of the Theoretical Astrophysics Center. Our thanks also go to Prof. Juri Toomre and Dr. Michael Knölker for hospitality at JILA and HAO respectively, during the time when much of this chapter was written.

## References

- Brown, T. M. (1985). *Nature* **317**, 591  
 Brown, T. M. and Morrow, C. A. 1987. *Astrophys. J.* **314**, L21  
 Brown, T. M., Christensen-Dalsgaard, J., Dziembowski, W. A., Goode, P., Gough, D. O. and Morrow, C. A. (1989). *Astrophys. J.* **343**, 526  
 Brun, A. S. and Toomre, J. (2001). *Astrophys. J.*, in the press  
 Chaplin, W. J., Christensen-Dalsgaard, J., Elsworth, Y., Howe, R., Isaak, G. R.,

- Larsen, R. M., New, R., Schou, J., Thompson, M. J. and Tomczyk, S. (1999). *Mon. Not. R. astr. Soc.* **308**, 405
- Charbonneau, P., Christensen-Dalsgaard, J., Henning, R., Larsen, R. M., Schou, J., Thompson, M. J. and Tomczyk, S. (1999). *Astrophys. J.* **527**, 445
- Christensen-Dalsgaard, J. and Schou, J. (1988). In *Seismology of the Sun & Sun-like Stars*, eds V. Domingo and E. J. Rolfe, ESA SP-286 (ESA Publications Division, Noordwijk, The Netherlands), 149
- Christensen-Dalsgaard, J., Däppen, W., Ajukov, S. V., Anderson, E. R., Antia, H. M., Basu, S., Baturin, V. A., Berthomieu, G., Chaboyer, B., Chitre, S. M., Cox, A. N., Demarque, P., Donatowicz, J., Dziembowski, W. A., Gabriel, M., Gough, D. O., Guenther, D. B., Guzik, J. A., Harvey, J. W., Hill, F., Houdek, G., Iglesias, C. A., Kosovichev, A. G., Leibacher, J. W., Morel, P., Proffitt, C. R., Provost, J., Reiter, J., Rhodes Jr., E. J., Rogers, F. J., Roxburgh, I. W., Thompson, M. J., Ulrich, R. K. (1996). *Science* **272**, 1286
- Corbard, T., Berthomieu, G., Morel, P., Provost, J., Schou, J. and Tomczyk, S. (1997). *Astron. Astrophys.* **324**, 298
- Corbard, T., Blanc-Féraud, L., Berthomieu, G. and Provost, J. (1999). *Astron. Astrophys.* **344**, 696
- Di Mauro, M. P. and Dziembowski, W. A. (1998). *Mem. Soc. Astron. Ital.* **69**, 559
- Duvall, T. L. (1995). In *Proc. Fourth SOHO Workshop: Helioseismology*, eds J. T. Hoeksema, V. Domingo, B. Fleck and B. Battrick, ESA SP-376, vol. 1 (ESA Publications Division, Noordwijk, The Netherlands), 107
- Duvall, T. L., Dziembowski, W. A., Goode, P. R., Gough, D. O., Harvey, J. W. and Leibacher, J. W. (1984). *Nature* **310**, 22
- Eff-Darwich, A. and Korzennik, S. G. (1998). In *Structure and dynamics of the interior of the Sun and Sun-like stars; Proc. SOHO 6/GONG 98 Workshop*, eds S. G. Korzennik and A. Wilson, ESA SP-418 (ESA Publications Division, Noordwijk, The Netherlands), 685
- Gilman, P. A. and Miller, J. (1986). *Astrophys. J. Suppl.* **61**, 585
- Gilman, P. A., Morrow, C. A. and DeLuca, E. E. (1989). *Astrophys. J.* **338**, 528
- Glatzmaier, G. (1985). *Astrophys. J.* **291**, 300
- Gough, D. O. (1976). In *Problems of stellar convection, IAU Colloq. No. 38, Lecture Notes in Physics*, vol. **71**, eds E. Spiegel and J.-P. Zahn (Springer-Verlag, Berlin), 15
- Gough, D. O. (1981). *Mon. Not. R. astr. Soc.* **196**, 731
- Gough, D. O. and McIntyre, M. E. (1998). *Nature* **394**, 755
- Gough, D. O. and Thompson, M. J. (1991). In *Solar interior and atmosphere*, eds A. N. Cox, W. C. Livingston and M. Matthews, Space Science Series (University of Arizona Press, Tucson, AZ), 519
- Gough, D. O. and Toomre, J. (1991). *Ann. Rev. Astron. Astrophys.* **29**, 627
- Haber, D. A., Hindman, B. W., Toomre, J., Bogart, R. S. and Hill, F. (2001). In *Helio- and Asteroseismology at the Dawn of the Millennium: Proc. SOHO 10 / GONG 2000 Workshop*, ed. A. Wilson, ESA SP-464 (ESA Publications Division, Noordwijk, The Netherlands), 213
- Hansen, C. J., Cox, J. P. and van Horn, H. M. (1977). *Astrophys. J.* **217**, 151
- Hart, J. E., Glatzmaier, G. A. and Toomre, J. (1986). *J. Fluid Mech.* **173**, 519
- Harvey, J. W., Hill, F., Hubbard, R. P., Kennedy, J. R., Leibacher, J. W., Pintar, J. A., Gilman, P. A., Noyes, R. W., Title, A. M., Toomre, J., Ulrich, R. K., Bhatnagar, A., Kennewell, J. A., Marquette, W., Partrón, J., Saá, O. and Yasukawa, E. (1996). *Science* **272**, 1284

- Howard, R. and LaBonte, B. J. (1980). *Astrophys. J.* **239**, L33
- Howe, R., Christensen-Dalsgaard, J., Hill, F., Komm, R. W., Larsen, R. M., Schou, J., Thompson, M. J. and Toomre, J. (2000a). *Astrophys. J.* **533**, L163
- Howe, R., Christensen-Dalsgaard, J., Hill, F., Komm, R. W., Larsen, R. M., Schou, J., Thompson, M. J., Toomre, J. (2000b). *Science* **287**, 2456
- Howe, R., Christensen-Dalsgaard, J., Hill, F., Komm, R. W., Larsen, R. M., Schou, J., Thompson, M. J. and Toomre, J. (2001). In *Helio- and Asteroseismology at the Dawn of the Millennium: Proc. SOHO 10 / GONG 2000 Workshop*, ed. A. Wilson, ESA SP-464 (ESA Publications Division, Noordwijk, The Netherlands), 19
- Ingersoll, A. P. (1990). *Science* **248**, 308
- Korzennik, S. G., Cacciani, A., Rhodes, E. J., and Ulrich, R. K. (1990). In *Progress of seismology of the sun and stars, Lecture Notes in Physics*, vol. **367**, eds Y. Osaki and H. Shibahashi (Springer-Verlag, Berlin), 341
- Kosovichev, A. G. (1996). *Astrophys. J.* **469**, L61
- Kosovichev, A. G. and Schou, J. (1997). *Astrophys. J.* **482**, L207
- Lada, C. J. and Shu, F. H. (1990). *Science* **248**, 564
- Libbrecht, K. G. (1988). In *Seismology of the Sun and Sun-like Stars*, eds V. Domingo and E. J. Rolfe, ESA SP-286, ESA Publications Division, Noordwijk, The Netherlands, 131
- Libbrecht, K. G. (1989). *Astrophys. J.* **336**, 1092
- Mestel, L. (1968). *Mon. Not. R. astr. Soc.* **138**, 359 – 391.
- Mestel, L. and Spruit, H. C. (1987). *Mon. Not. R. astr. Soc.* **226**, 57 – 66.
- Miesch, M. S. (2000). *Solar Phys.* **192**, 59
- Miesch, M. S., Elliott, J. R., Toomre, J., Clune, T. L., Glatzmaier, G. A. and Gilman, P. A. (2000). *Astrophys. J.* **532**, 593
- Pidatella, R. M., Stix, M., Belvedere, G. and Paterno, L. (1986). *Astron. Astrophys.* **156**, 22
- Pinsonneault, M. H., Kawaler, S. D., Sofia, S. and Demarque, P. (1989). *Astrophys. J.* **338**, 424
- Scherrer, P. H., Bogart, R. S., Bush, R. I., Hoeksema, J. T., Kosovichev, A. G., Schou, J., Rosenberg, W., Springer, L., Tarbell, T. D., Title, A., Wolfson, C. J., Zayer, I., and the MDI engineering team (1995). *Solar Phys.* **162**, 129
- Schou, J., Antia, H. M., Basu, S., Bogart, R. S., Bush, R. I., Chitre, S. M., Christensen-Dalsgaard, J., Di Mauro, M. P., Dziembowski, W. A., Eff-Darwich, A., Gough, D. O., Haber, D. A., Hoeksema, J. T., Howe, R., Korzennik, S. G., Kosovichev, A. G., Larsen, R. M., Pijpers, F. P., Scherrer, P. H., Sekii, T., Tarbell, T. D., Title, A. M., Thompson, M. J., Toomre, J. (1998). *Astrophys. J.* **505**, 390
- Schou, J. (1999). *Astrophys. J.* **523**, L181
- Schou, J., Christensen-Dalsgaard, J. and Thompson, M. J. (1994). *Astrophys. J.* **433**, 389
- Skumanich, A. (1972). *Astrophys. J.* **171**, 565
- Snodgrass, H. B. and Ulrich, R. K. (1990). *Astrophys. J.* **351**, 309
- Spiegel, E. A. and Zahn, J.-P. (1992). *Astron. Astrophys.* **265**, 106
- Stein, R. F. and Nordlund, Å. (1989). *Astrophys. J.* **342**, L95
- Stein, R. F. and Nordlund, Å. (1998). *Astrophys. J.* **499**, 914
- Thompson, M. J., Toomre, J., Anderson, E. R., Antia, H. M., Berthomieu, G., Burtonclay, D., Chitre, S. M., Christensen-Dalsgaard, J., Corbard, T., DeRosa, M., Genovese, C. R., Gough, D. O., Haber, D. A., Harvey, J. W.,

- Hill, F., Howe, R., Korzennik, S. G., Kosovichev, A. G., Leibacher, J. W., Pijpers, F. P., Provost, J., Rhodes Jr., E. J., Schou, J., Sekii, T., Stark, P. B. and Wilson, P. R. (1996). *Science* **272**, 1300
- Tomczyk, S., Schou, J. and Thompson, M. J. (1995). *Astrophys. J.* **448**, L57